Clim Dyn (2009) 32:799–815
DOI 10.1007/s00382-008-0509-0

A comparison of PMIP2 model simulations and the MARGO proxy reconstruction for tropical sea surface temperatures at last glacial maximum

Bette L. Otto-Bliesner · Ralph Schneider · E. C. Brady · M. Kucera · A. Abe-Ouchi · E. Bard · P. Braconnot · M. Crucifix · C. D. Hewitt · M. Kageyama · O. Marti · A. Paul · A. Rosell-Melé · C. Waelbroeck · S. L. Weber · M. Weinelt · Y. Yu

Received: 5 November 2007 / Accepted: 10 December 2008 / Published online: 20 January 2009

Abstract Results from multiple model simulations are used to understand the tropical sea surface temperature (SST) response to the reduced greenhouse gas concentrations and large continental ice sheets of the last glacial maximum (LGM). We present LGM simulations from the Paleoclimate Modelling Intercomparison Project, Phase 2 (PMIP2) and compare these simulations to proxy data collated and harmonized within the Multiproxy Approach for the Reconstruction of the Glacial Ocean Surface Project (MARGO). Five atmosphere–ocean coupled climate models (AOGCMs) and one coupled model of intermediate complexity have PMIP2 ocean results available for LGM. The models give a range of tropical (defined for this paper as 15°S–15°N) SST cooling of 1.0–2.4°C, comparable to the MARGO estimate of annual cooling of 1.7 ± 1°C. The models simulate greater SST cooling in the tropical Atlantic than tropical Pacific, but interbasin and intrabasin variations of cooling are much smaller than those found in the MARGO reconstruction. The simulated tropical coolings are relatively insensitive to season, a feature also present in the MARGO transferred-based estimates calculated from planktonic foraminiferal assemblages for the Indian and Pacific Oceans. These assemblages indicate seasonality in cooling in the Atlantic basin, with greater

B. L. Otto-Bliesner (✉) · E. C. Brady
Climate and Global Dynamics Division, National Center for Atmospheric Research, Boulder, CO, USA
e-mail: ottobli@ucar.edu

R. Schneider · M. Weinelt
Institut für Geowissenschaften,
Christian-Albrechts Universität, Kiel, Germany

M. Kucera
Institut für Geowissenschaften,
Eberhard-Karls Universität Tübingen, Tübingen, Germany

A. Abe-Ouchi
Center for Climate System Research, The University of Tokyo, Kashiwa, Japan

E. Bard
CEREGE, College de France, CNRS, Universite Aix-Marseille, Europôle de l'Arbois, Aix-en-Provence, France

P. Braconnot · M. Kageyama · O. Marti · C. Waelbroeck
Laboratoire des Sciences du Climat et de l'Environnement,
Unité mixte CEA-CNRS-UVSQ,
Gif-sur-Yvette Cedex, France

M. Crucifix
Institut d'Astronomie et de Géophysique Georges Lemaître,
Université Catholique de Louvain,
Louvain-la-Neuve, Belgium

C. D. Hewitt
Met Office Hadley Centre, Exeter, UK

A. Paul
Department of Geosciences,
Bremen University, Bremen, Germany

A. Rosell-Melé
ICREA and Institut de Ciencia i Tecnologia Ambientals,
Universitat Autònoma de Barcelona,
Barcelona, Spain

S. L. Weber
Royal Netherlands Meteorological Institute (KNMI),
De Bilt, The Netherlands

Y. Yu
LASG, Institute of Atmospheric Physics,
Chinese Academy of Sciences, Beijing,
People's Republic of China

cooling in northern summer than northern winter, not captured by the model simulations. Biases in the simulations of the tropical upwelling and thermocline found in the preindustrial control simulations remain for the LGM simulations and are partly responsible for the more homogeneous spatial and temporal LGM tropical cooling simulated by the models. The PMIP2 LGM simulations give estimates for the climate sensitivity parameter of 0.67°–0.83°C per Wm^{-2}, which translates to equilibrium climate sensitivity for doubling of atmospheric CO_2 of 2.6–3.1°C.

Keywords Last glacial maximum · MARGO · PMIP · Tropical oceans · Climate sensitivity

1 Introduction

The tropical oceans play a key role in the global heat and moisture budgets. It is important, therefore, to understand the sensitivity of tropical oceans to climate change. The last glacial maximum (LGM) is a recent past time period to consider the sensitivity to the lower glacial CO_2 levels. The magnitudes and patterns of tropical glacial cooling of the oceans have been debated for a number of years. In the early 1980s, the CLIMAP (Climate: Long-Range Investigation, Mapping, and Prediction) project produced a reconstruction of ~1–2°C SST cooling over large parts of the oceans but with modest warming in the subtropical gyres of the North and South Pacific (CLIMAP project members 1981). Mix and collaborators (Mix et al. 1999) estimated pronounced glacial cooling from their foraminiferal assemblages with cooling of 5–6°C in the equatorial current systems of the Atlantic and eastern Pacific Oceans. Recent reconstructions confirm moderate cooling, mostly in the range of 0–4°C, of tropical SSTs, although with significant regional variation and greater cooling in the eastern Atlantic and Pacific Oceans (Pflaumann et al. 2003; Rosell-Mele et al. 2004; Barker et al. 2005; Barrows and Juggins 2005; Chen et al. 2005; Kucera et al. 2005b). Based on an objective approach incorporating a variety of marine proxies and including measures of the precision of these proxies, Ballantyne et al. (2005) estimated LGM SST cooling over the tropical ocean basin from 30°S–30°N of 2.7 ± 0.5°C (±σ), with regional tropical coolings of 3°C in the Atlantic, 2.5°C in the Indian, and 1°C in the central Pacific Oceans. Less LGM tropical cooling of 1.7°C and 1.5°C for 15°S–15°N and 30°S–30°N, respectively, with a total error of 1 and 1.2°C, respectively, was obtained in the analysis of the multi-proxy MARGO data (MARGO Project Members 2009).

Atmospheric model simulations as part of PMIP1, using the CLIMAP boundary conditions over land and slab ocean models with ocean heat transports prescribed from modern, produced a cooling of tropical SSTs (30°S–30°N) of 0.8–3.4°C (Pinot et al. 1999). The cooling predicted by the PMIP1 slab ocean models is greater than that of the CLIMAP reconstruction, particularly over the Pacific and Indian Oceans. The first simulations of LGM with coupled ocean-atmosphere models produced a wider range of cooling of the tropical oceans as compared to modern from moderate cooling of 1.5–3°C (Hewitt et al. 2001; Kitoh and Murakami 2002; Shin et al. 2003) to strong cooling of 4.5°C (Peltier and Solheim 2004) and 6.5°C (Kim et al. 2003). The varying forcings and boundary conditions of these LGM simulations make it difficult to separate the cooling due to different model sensitivities from the cooling resulting from different forcings and boundary conditions.

The second phase of the Paleoclimate Modeling Intercomparison Project (PMIP2) defined a common set of forcings and boundary conditions for LGM and preindustrial conditions for coupled atmosphere-ocean models to improve comparison among models and with data and to provide a benchmark for simulations being used for future climate change projections (Braconnot et al. 2007). In this paper, we compare the predictions of tropical sea surface temperatures for the last glacial maximum from six atmosphere-ocean models to the data synthesis of MARGO to test whether coupled climate models are able to produce observed conditions in a past climate situation very different from today. The model results are evaluated in terms of their regional, seasonal, and depth variations of glacial cooling. We also include a discussion of global climate sensitivity using the predicted LGM cooling estimates by the PMIP2 models.

2 The models

Coupled atmosphere-ocean model simulations for LGM and preindustrial (PI) conditions are available from the PMIP2 international project [http://pmip2.lsce.ipsl.fr] (Braconnot et al. 2007). The models included in this paper are CCSM (the National Center for Atmospheric Research CCSM3 model), FGOALS (the LASG/IAP FGOALS-g1.0 model), HadCM (the UK Met Office Hadley Centre HadCM3 model with MOSES2 surface scheme), IPSL (the Institut Pierre Simon Laplace IPSL-CM4 model), MIROC (the CCSR/NIES/FRCGC MIROC3.2.2 (medres) model), and ECBilt-CLIO (the Royal Netherlands Meteorological Institute ECBilt/the Louvain-la neuve CLIO intermediate-complexity model). Details can be found in Table 1.

The PMIP2 simulations used the same models as being used for the future scenario projections of the IPCC Fourth Assessment Report (AR4), except for changes as noted in

Table 1 Details of PMIP2 models with LGM simulations

Model reference	Sponsor(s), Country	Atmosphere resolution	Ocean resolution in tropics (lat × long)	Differences from IPCC future scenario simulations
Coupled climate models				
CCSM3 (Otto-Bliesner et al. 2006a; Otto-Bliesner et al. 2006b)	National Center for Atmospheric Research, USA	T42 (2.8° × 2.8°)	0.3–1° × 1°	IPCC simulations at higher atmospheric model resolution
FGOALS-g1.0 (Yu et al. 2004)	LASG/Institute of Atmospheric Physics, China	T42 (2.8° × 2.8°)	1° × 1°	None
HadCM3M2 (Gordon et al. 2000)	UK Met Office Hadley Centre, UK	2.5° × 3.8°	1.25° × 1.25°	IPCC simulations use different land surface scheme
IPSL-CM4 (Marti et al. 2005)	Institut Pierre Simon Laplace, France	2.5° × 3.75°	1–2° × 2°	None
MIROC3.2(medres) (Developers K-1 2004)	Center for Climate System Research (University of Tokyo), National Institute for Environmental Studies, and Frontier Research Center for Global Change (JAMSTEC), Japan	T42 (2.8° × 2.8°)	0.5–1.4° × 1.4°	IPCC simulations run at both medres and hires
Coupled model of intermediate complexity				
ECBilt-CLIO (Weber and Drijhout 2007)	Royal Netherlands Meteorological Institute, The Netherlands and Louvain-La-Neuve, Belgium	T21 (5.6° × 5.6°) Quasi-geostrophic	3° × 3°	IPCC simulations use interactive vegetation scheme

Differences between PMIP2 and IPCC model configurations are listed in last column

Table 1 and as follows. CCSM used for AR4 future scenario simulations had an atmosphere resolution of T85; CCSM used for PMIP2 had an atmosphere resolution of T42. Both used the same ocean resolution. The MIROC model used for PMIP2 is the MIROC3.2-medres model, with an atmosphere resolution of T42, one of the resolutions used for AR4 future scenario simulations, and included for the PMIP2 LGM simulation a small fix to the bulk coefficient to the ice sheet. HadCM used for PMIP2 included a different land surface scheme, MOSES2, than the version used for AR4 future scenario simulations. ECBilt-CLIO AR4 scenario runs included interactive vegetation (VECODE), while the model version used for PMIP2 had vegetation fixed at modern and applied a local freshwater correction in the South Atlantic (run S, Weber and Drijhout 2007).

PMIP2 established standard forcings and boundary conditions for the LGM and PI to allow more rigorous comparisons among the models (Table 2). The PI simulations used forcings appropriate for conditions before industrialization, ca. 1750 AD, and the LGM simulations used forcings reconstructed for ~21,000 years ago (21 ka). The CCSM and HadCM simulations started from the cold state of previous LGM coupled simulations. The other LGM simulations were initialized from modern conditions. The LGM simulations of all models were run sufficiently long such that trends in temperatures are small (Braconnot et al. 2007).

Table 2 PMIP2 forcings and boundary conditions for LGM and preindustrial simulations

	LGM	Preindustrial
Greenhouse gases		
Carbon dioxide (ppmv)	185	280
Methane (ppbv)	350	760
Nitrous oxide (ppbv)	200	270
Orbital	21,000 year BP	1950 AD[a]
Eccentricity	0.018994	0.16724
Obliquity (°)	22.949	23.446
Angular precession (°)	114.42	102.04
Ice sheets	ICE-5G	Present-day
Land-sea mask	ICE-5G	Present-day
Vegetation	Present-day	Present-day

[a] The orbital parameters for the preindustrial control simulation are prescribed to the reference values of 1950 AD, as done in PMIP1. The differences in 1750 and 1950 insolation induced by changes in the orbital parameters are negligible

The PMIP2 boundary conditions for the LGM simulations are the ICE-5G ice sheet and topography (Peltier 2004) and the specification of additional land due to the lowering of sea level with the large amounts of water frozen in the continental ice sheets. The lowering of sea level results in exposed land in the tropics, most notably through the Indonesian Archipelago and between Australia and New Guinea. The present-day river routings were used in all of the LGM simulations except for those with HadCM and ECBilt-CLIO. These two models altered the river pathways in regions that are covered by the ICE-5G ice sheets during the LGM (see Weber et al. 2007 for more details). Vegetation and dust aerosols are unchanged from the PI control simulation.

The forcings for LGM relative to PI are the small change to insolation resulting from the slightly different Earth's orbit, which is set appropriate for 21 ka based on the calculations of Berger (1978), and the reduced concentrations of atmospheric carbon dioxide (CO_2), methane (CH_4), and nitrous oxide (N_2O) (Table 2), as adopted from the Greenland and Antarctic ice core records (Flückiger et al. 1999; Dallenbach et al. 2000; Monnin et al. 2001).

3 The data

The PMIP2 model simulations are compared to a proxy reconstruction of LGM tropical sea surface temperatures from the MARGO project, which includes both microfossils and geochemical approaches [http://margo.pangaea.de] (Kucera et al. 2005a). Following the EPILOG recommendation (Mix et al. 2001), MARGO adopted the period of 23–19 ka as the dating criteria for a marine proxy record to be included into the LGM synthesis. This is the period of maximum glacial sea level low stand on the north Australian shelf (Fleming et al. 1998; Yokoyama et al. 2000) and corresponds to continental LGM reconstructions (Farrera et al. 1999; Peltier 2004). Coretop samples do not necessarily represent present-day but rather, depending on sedimentation rates, decades to thousands of years within the Holocene (Kucera et al. 2005b).

The tropical (15°S–15°N) reconstruction of LGM SST from MARGO includes estimates from 156 marine sediment records based on planktonic foraminifera transfer functions (126 estimates), alkenones (32 estimates) and Mg/Ca (18 estimates). In this paper, all estimates are considered to represent annual-average SSTs although Mg/Ca is known to reflect the calcification temperature of the species on which it is measured, which appears best represented by the warm season SST (Barker et al. 2005). All proxies were calibrated on the 10 m World Ocean Atlas 1998 SST (Levitus et al. 1998) using the same definition of caloric seasons (Kucera et al. 2005a). Most of the tropical oceans are covered by at least one type of proxy. The eastern tropical Pacific and Atlantic, the Caribbean, and parts of the Indian Ocean are covered by multiple proxies (Fig. 1).

Uncertainties in the various proxy estimates exist for a number of reasons (see (Bard 2001; Kucera et al. 2005a) for further discussion). The proxy estimates depend on the ecology and biology of each source organism and may depend on more than one climatic parameter. Statistical approaches are required to empirically calibrate the proxies assuming the present-day spatial variation of the target environmental parameters can be used to reconstruct its temporal variation for the past. In addition, some proxies are known to have lower reliability in, for example, low salinity environments (alkenones, e.g. Bendle and Rosell-Mele 2004) and upwelling regions (Kucera et al. 2005b). Dissolution of foraminiferal calcite at the sea-floor can also bias Mg/Ca estimates to be too cold (Barker et al. 2005).

Changes in the depth habitat of the source organism and the season(s) its chemistry is recording remain a matter of some debate. Foraminiferal species live at various depths in the water column and their preferred habitat might vary for past oceanographic conditions. Mg/Ca estimates are from foraminifer species that dwell at mixed-layer depths (Barker et al. 2005). In the presence of a strong variation in productivity linked to upwelling, foraminiferal assemblages in the tropics may be biased towards the environmental conditions prevailing during the production time, e.g. the upwelling season. These factors are captured by the transfer functions, but only within the limits of the present-day range of equatorial upwelling variability. If this was higher during the LGM, the assemblages thus produced would lack an appropriate representation in the calibration dataset and the estimates based on those fossil faunas may thus be misleading. The presence of such no-analog situations can be detected by various techniques and Kucera et al. (2005b) note a significant level of uncertainty associated with the extremely cold estimates in the eastern tropical Pacific.

Alkenones, are expected to consistently represent "real" sea surface temperature as they are produced by phytoplankton, which can also be derived from the sediment calibration of the proxy against SSTs at 0 m depth (Mueller et al. 1998). In fact the alkenone signal originates in the surface mixed layer, and on occasion in the deep chlorophyll maximum (Conte et al. 2001; Lee and Schneider 2005; Prahl et al. 2005). Environmental preferences of alkenone producing algae may bias them towards warmer temperatures, particularly in regions where both upwelling and open ocean conditions alternately affect sites (Niebler et al. 2003). Locally their signal is also strongly seasonal with a strong interannual variability (e.g., (Conte et al. 1998; Mueller and Fischer 2001).

4 Results

4.1 Tropical sea surface temperatures simulated by PMIP2 models

The overall characteristics of the tropical SSTs for PI are well depicted in the multi-model mean (Fig. 2). Warmest

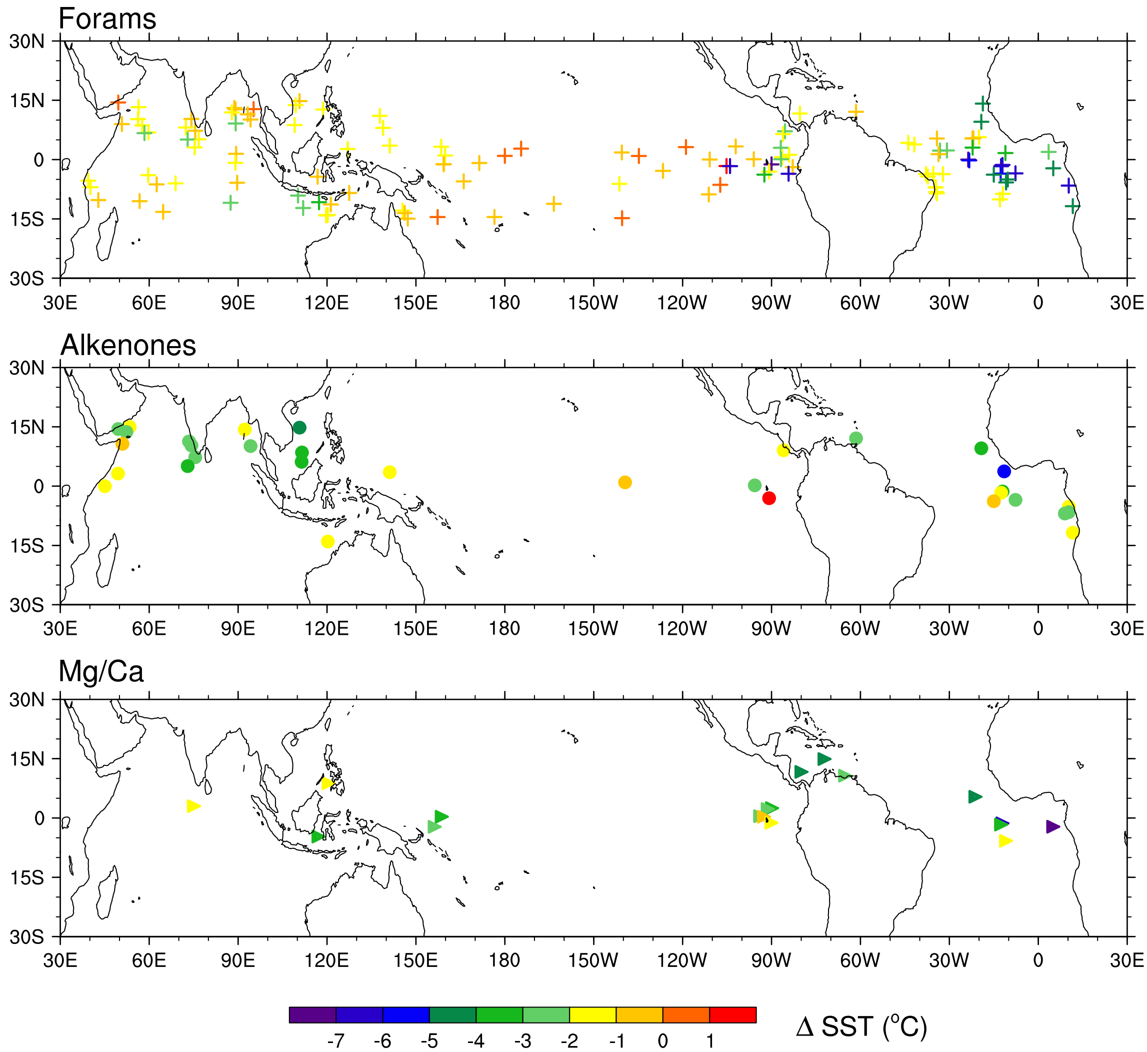

Fig. 1 Proxy estimates of LGM sea surface temperature change (°C) based on foraminifera transfer functions (top), alkenones (middle), and foraminifera Mg/Ca (bottom) in MARGO synthesis (http://margo.pangaea.de)

tropical SSTs (>28°C) occur in the Western Pacific Warm Pool (WPWP, approximately 100°E longitude to the dateline) and in the Indian Ocean. The equatorial cold tongue in the central and eastern Pacific is also simulated, though extends too far westward. The major discrepancies between simulated and observed tropical SSTs occur in the upwelling regions along the western coasts of South America and Africa. Simulated SSTs in these regions are generally 2–4°C too warm compared to observed. These biases occur in each of the models included in this study (Fig. 2). The model simulations are unable to capture the narrow zones of eastern boundary currents and coastal upwelling in the eastern basins of the subtropical south Atlantic and Pacific (more details in Sect. 4.4).

Figure 3 and Table 3 give the annual mean SST changes, LGM minus PI, simulated by the PMIP2 models. The ECBilt-CLIO intermediate complexity model simulates the weakest cooling of the tropical oceans at LGM with average cooling of 1.0°C. The five AOGCMs define a relatively similar range of tropical ocean cooling of 1.7–2.4°C. All models simulate greater mean cooling of SSTs in the tropical Atlantic than the tropical Pacific (Table 3). Basin-mean Indian Ocean SSTs show cooling in the range from 1.1–2.5°C in the PMIP2 models (Table 3).

4.2 MARGO reconstruction of LGM sea surface temperatures

Environmental calibration of planktonic foraminifera (assemblages) census counts provides the largest data set for reconstruction of tropical sea surface temperatures (Kucera et al. 2005b) (Fig. 1). Foraminiferal assemblages indicate 0–2°C cooling over much of the tropical oceans at LGM but with some notable spatial exceptions. In the

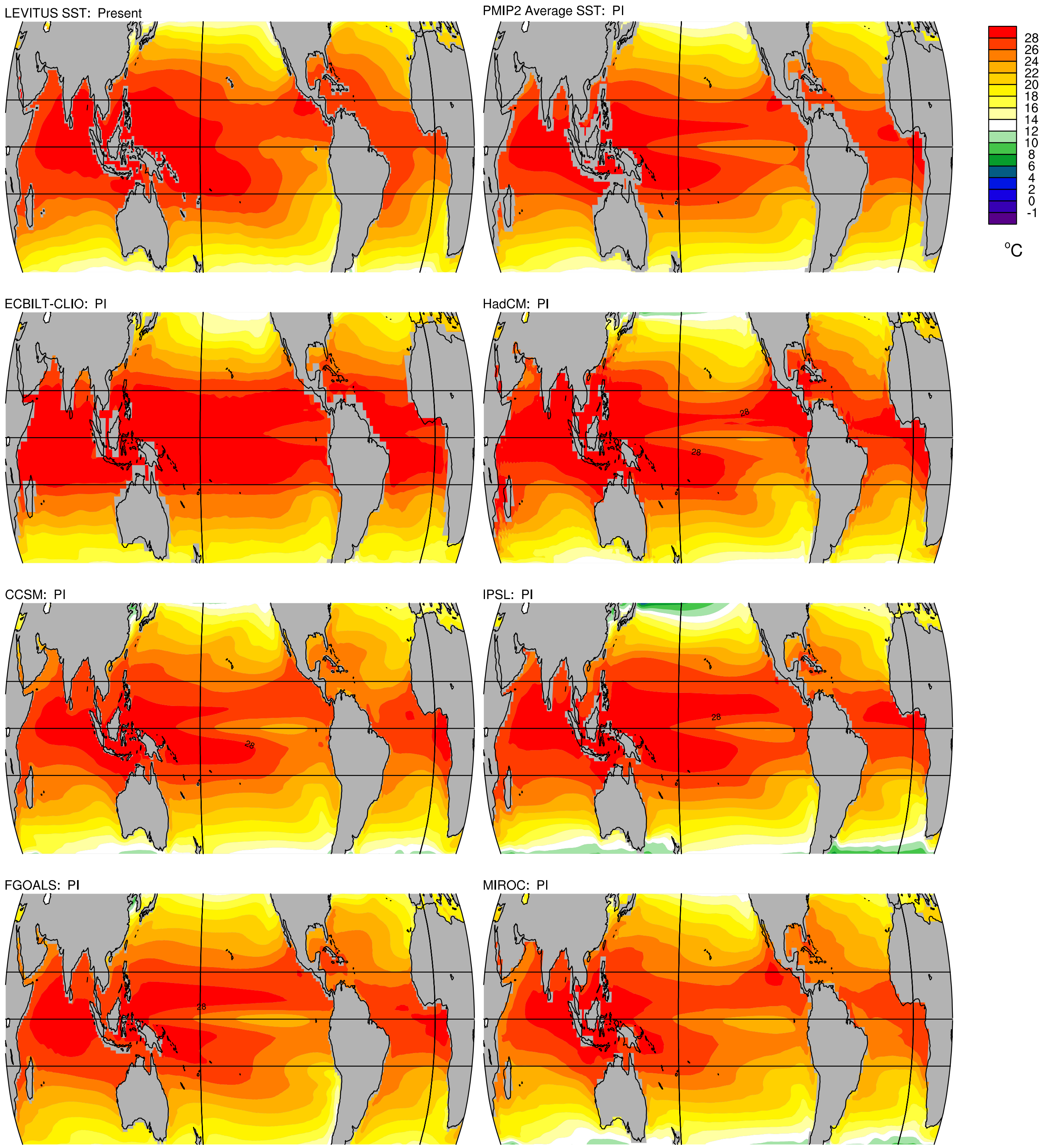

Fig. 2 Sea surface temperatures (°C) for observed present-day (Levitus et al. 1998), PMIP2 preindustrial multi-model mean, and PMIP2 preindustrial simulations of individual models. *Black horizontal lines* delineate latitudes 15°S, equator and 15°N

eastern tropical Atlantic, east of 25°W, many cores indicate LGM cooling in excess of 3°C with some cores indicating LGM cooling of 5°C or greater. Cooling in the western tropical Atlantic warm pool is only 1–2°C. In the eastern tropical Pacific, foraminiferal assemblages suggest cooling of less than 3°C at most sites, although a few cores indicate cooling in excess of 6°C. Estimates of cooling in the WPWP are 1–2°C (Chen et al. 2005). Several cores in the central tropical Pacific show little or no cooling at LGM as compared to modern. Moderate cooling of 2–3°C is

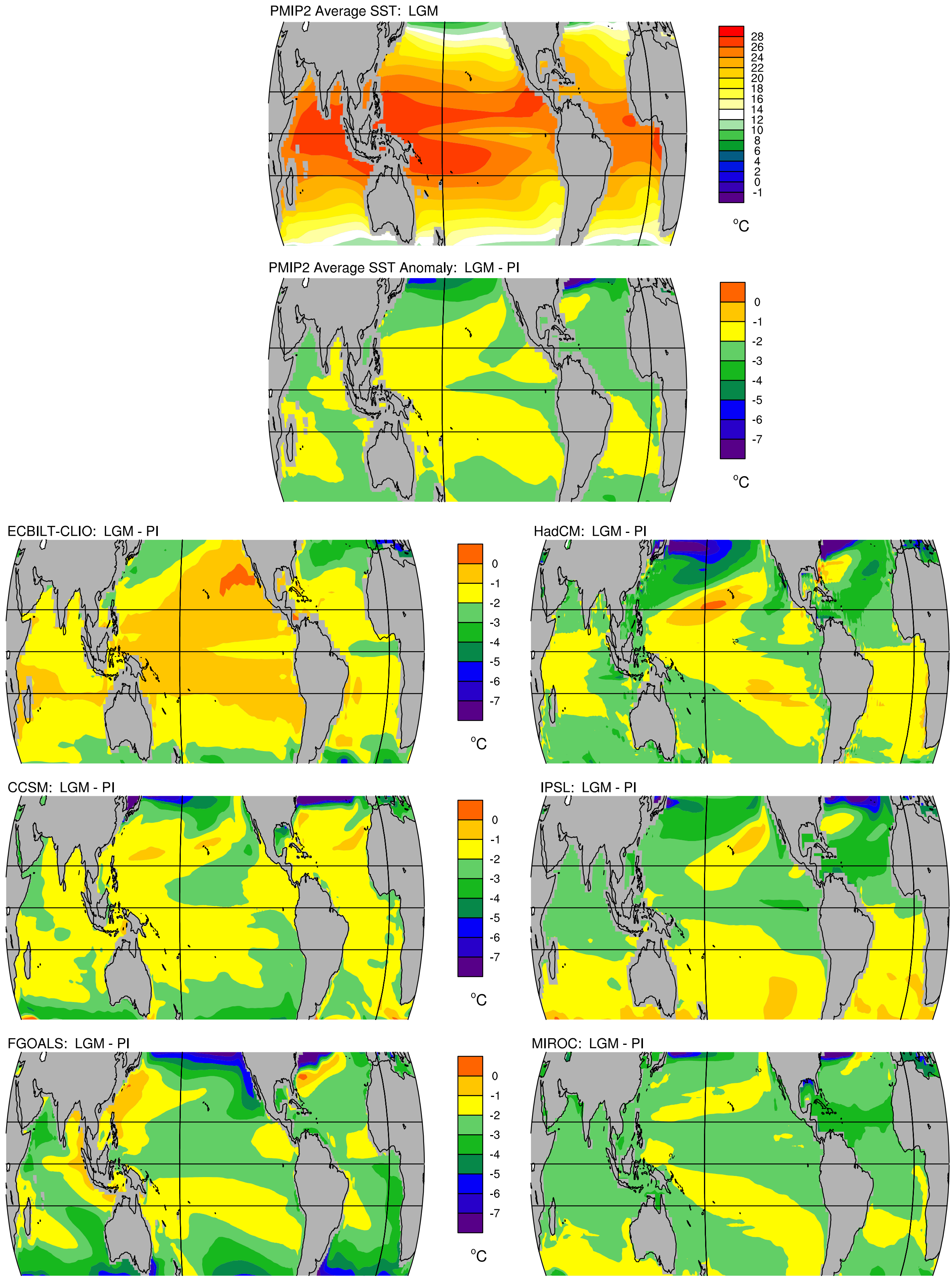

Fig. 3 Sea surface temperature (°C). Top two panels show the multi-model mean LGM SST and SST change, LGM minus PI. Also shown are the SST change, LGM minus PI, simulated by each of the six PMIP2 models. *Black horizontal lines* delineate latitudes15°S, equator and 15°N

Table 3 Annual mean changes of sea surface temperature (SST), LGM minus PI, as simulated by the PMIP2 models and estimated from the MARGO data

	ΔSST LGM 15°S–15°N All basins	ΔSST LGM 15°S–15°N Indian[a]	ΔSST LGM 15°S–15°N Pacific[b]	ΔSST LGM 15°S–15°N Atlantic[c]
MARGO data	−1.7 ± 1	−1.4 ± 0.7	−1.2 ± 1.1	−2.9 ± 1.3
ECBilt-CLIO	−1.0	−1.1	−0.8	−1.5
CCSM	−1.7	−1.8	−1.6	−1.8
FGOALS	−2.2	−1.9	−2.3	−2.4
HadCM	−2.0	−2.2	−1.7	−2.0
IPSL	−2.3	−2.2	−2.2	−2.3
MIROC	−2.4	−2.5	−2.2	−2.6

The MARGO values are regional mean anomalies based on block-averaged data with reliability weighting. Error estimates are total error, with this error assessment including calibration errors, samples per core, and age model quality. Details of the MARGO calculations can be found in MARGO Project Members (2009). Units are °C

[a] 20°E–150°E

[b] 150°E–70°W

[c] 70°W–20°E

indicated for some cores in the eastern Indian Ocean, particularly south of the Indonesian Archipelago (Barrows and Juggins 2005).

Much fewer estimates of LGM SST changes for the tropical oceans are available from alkenones and Mg/Ca (Fig. 1). Estimates from alkenones and Mg/Ca give a similar picture of cooling in much of the eastern tropical Atlantic as the foraminiferal transfer-based reconstruction, with the greatest disagreements seen in the upwelling regions off Africa (Niebler et al. 2003). As compared to the foraminiferal assemblage estimates, SST estimates from alkenones and Mg/Ca show greater cooling in the Caribbean (both proxies), northern Indian Ocean (alkenones), and WPWP (Mg/Ca). The Mg/Ca estimates indicate similar cooling of about 2–3°C in the eastern and western tropical Pacific, while foraminiferal assemblages suggest cooling of less than 2°C in the western Pacific. All three proxies indicate significant local gradients of cooling in the easternmost tropical Pacific attesting to the complex oceanographic conditions in this region. Differences in depth habitat, nutrients, season of production, and dissolution effects will need to be better understood to explain the different ice-age cooling signals estimated from each of the proxies for paleotemperature in the eastern equatorial Pacific (Mix 2006).

4.3 Comparison of LGM cooling: PMIP2 simulations and MARGO reconstruction

The PMIP2 models estimate an annual average tropical cooling from 15°N–15°S in the range of 1–2.4°C (Table 3), which compares well to the estimate from the MARGO reconstruction of 1.7 ± 1°C (MARGO Project Members 2008). The models however, simulate a more uniform distribution of cooling compared to the distinct interbasin differences evident in the proxy estimates (Figs. 1 and 3). ECBILT simulates the least cooling and MIROC the most cooling, but the degree of cooling remains relatively similar across the Indian, Pacific, and Atlantic Ocean basins in each PMIP2 model (Table 3). The zonal uniformity of the model predicted LGM cooling suggests that there is not a significant change to the spatial gradients of temperature simulated by the models. This is a robust result across all models. On the other hand, interpretation of MARGO results (Kucera et al. 2005b) find that some of the spatial patterns in the observed tropical LGM cooling estimates are consistent across different cores and proxy types and may reflect changes in ocean circulation.

To better compare the model output to the proxies, the simulated temperatures are sampled and plotted at the same locations as the MARGO estimates from assemblages of planktonic forameninfera (Figs. 1, 4 and 5). This provides a first-order comparison of the predicted versus observed SST changes over the three ocean basins; better estimates of the regional cooling would need to consider the spatial sampling and proxy uncertainties. The PMIP2 models simulate LGM cooling of tropical SSTs with little intrabasin variations in cooling across the tropical oceans. This contrasts with the proxy data, which indicates much greater cooling (in excess of 4°C at many cores) in the eastern half of the tropical Atlantic and very little cooling in the central Pacific region between the 180° and 120°W longitude, intrabasin differences that are considered robust (Kucera et al. 2005b). The proxy data has greater LGM cooling in the eastern Pacific at three sites but absent these estimates, the cooling in the eastern Pacific cold tongue and western Pacific warm pool are similar (Fig. 4). Although one model simulation might agree better than the other model simulations in a specific tropical ocean region, this agreement is fortuitous, being the result of greater or lesser overall sensitivity to the forcing, rather than correctly simulating the varying longitudinal and seasonal contributions of radiative and dynamic factors to cooling of the tropical oceans (see next sections).

4.4 Sensitivity of tropical ocean cooling with depth

The LGM cooling estimated from the MARGO reconstruction of SST from assemblages of planktonic foraminifera shows that the eastern half of the tropical Atlantic basin is at least 2°C cooler than the western half. One explanation for the failure of the models to simulate the regional LGM

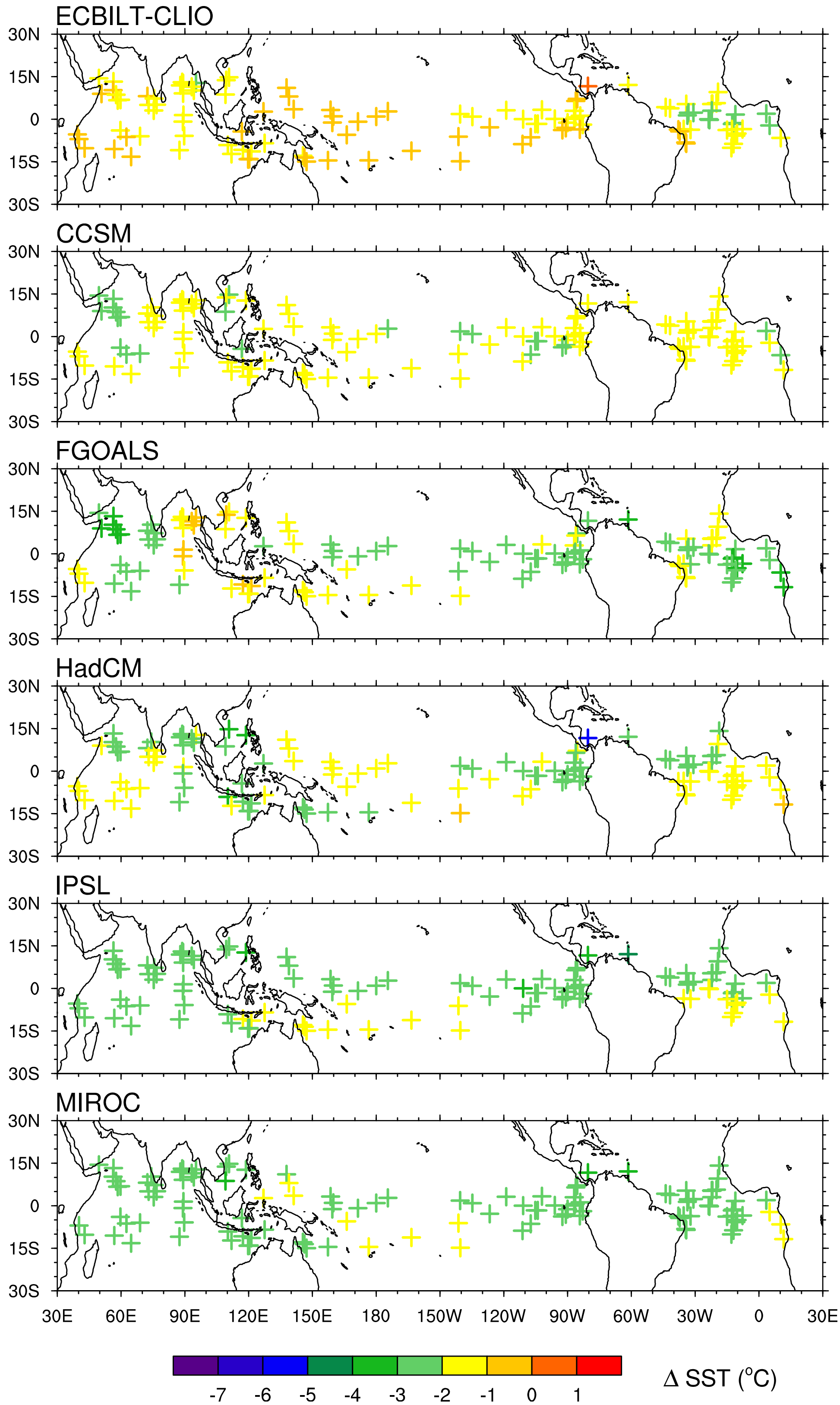

Fig. 4 LGM sea surface temperature change as simulated by the PMIP2 models at locations of proxy estimates based on the foraminifera transfer functions (MARGO Project Members 2009)

surface cooling patterns evident in the proxy data is that models have known regional biases in the simulations of equatorial (5°S–5°N) upper ocean temperature structure in PI simulations (Fig. 6). These biases are related to deficiencies that are evident in all the PMIP2 climate models and remain in the LGM simulations.

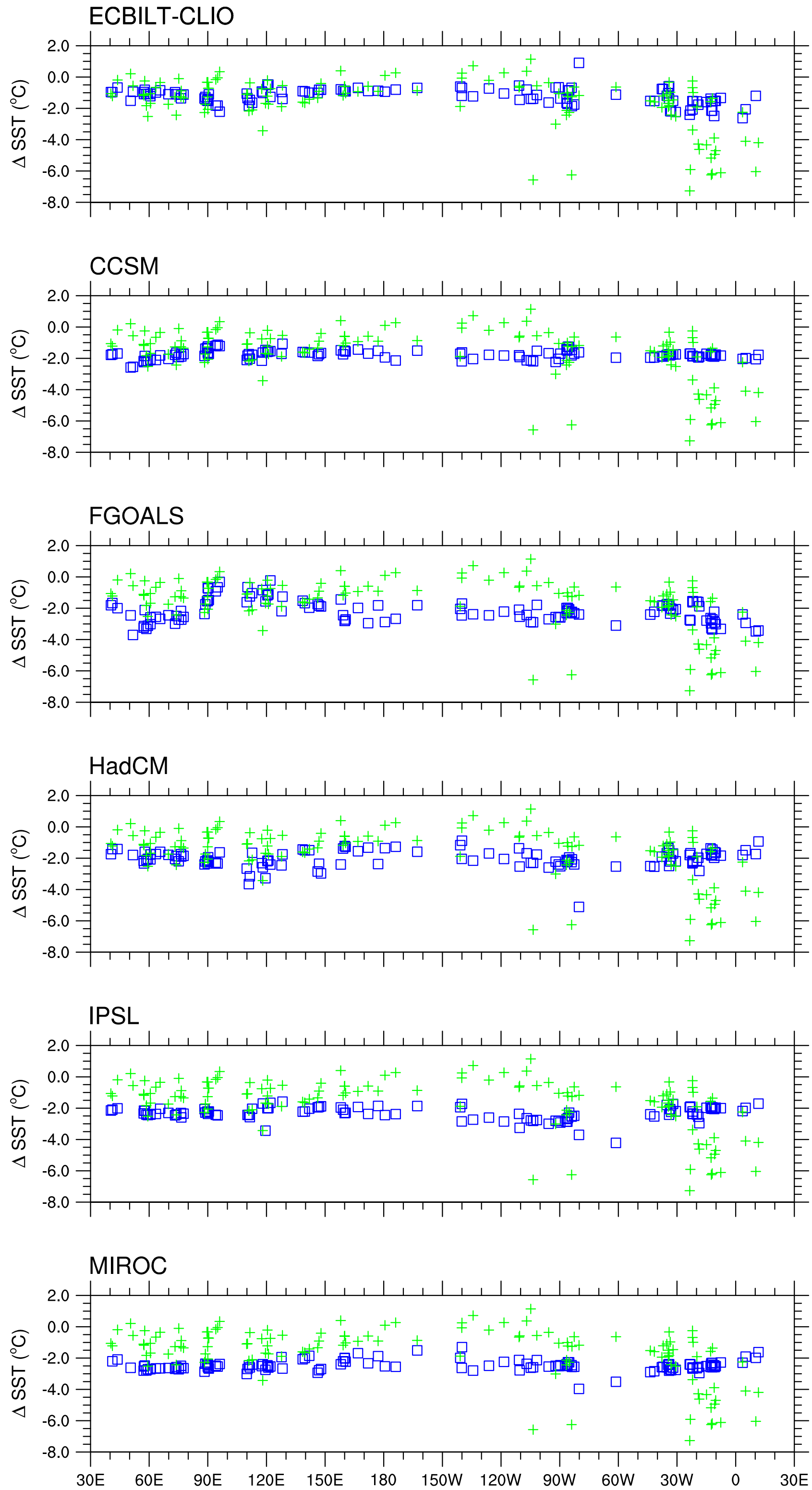

Fig. 5 Tropical (15°S–15°N) SST anomaly, LGM minus PI, simulated by the PMIP2 models (*square boxes*) at the locations of proxy estimates based on the foraminifera transfer functions as compared to the proxy estimates (*plus*), (MARGO Project Members 2009). Site V21-30 in eastern Pacific with LGM cooling estimate of −10.6°C is not plotted

In the equatorial Atlantic Ocean, the control PI simulations from all the models show large warm biases in surface and upper ocean temperatures in the eastern portions that manifests as flatter or deeper than observed thermoclines. Upper ocean warm biases are also evident near the eastern boundary of the tropical Pacific basin in the PMIP2 model PI simulations. Results from detailed analyses of CCSM have attributed these biases to resolution and physics. Deser et al. (2006) suggest that the lack of a cold tongue in the Atlantic basin in the CCSM3 is

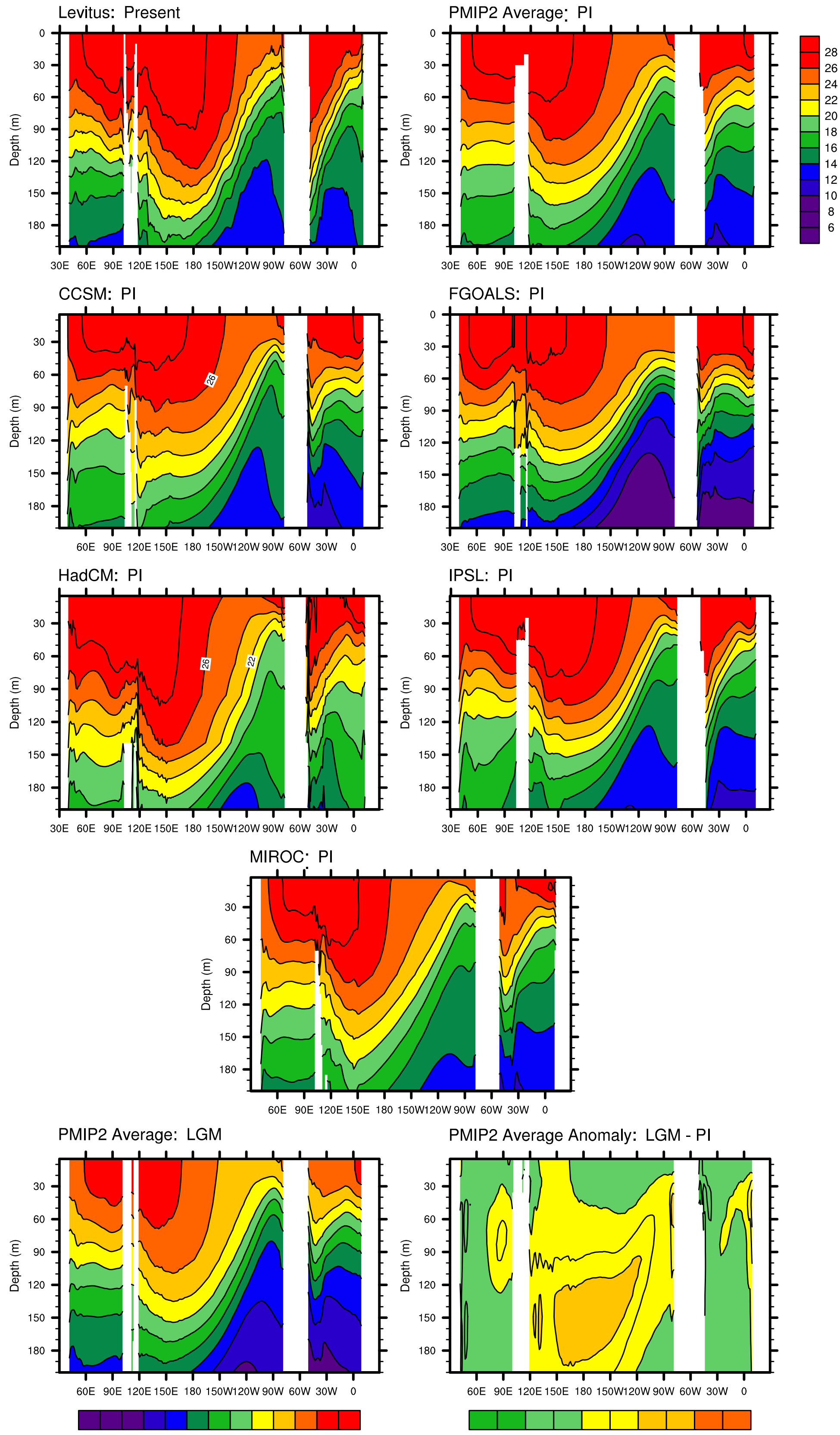

Fig. 6 Equatorial (5°N–5°S) ocean temperatures (°C) in top 200 m of the ocean. Top two panels show the observed present-day (Levitus et al. 1998) and PMIP2 preindustrial multi-model mean. Middle panels show the simulated temperatures from the PMIP2 preindustrial simulations of the individual models. Bottom two panels show the multi-model mean LGM temperature and temperature change, LGM minus PI

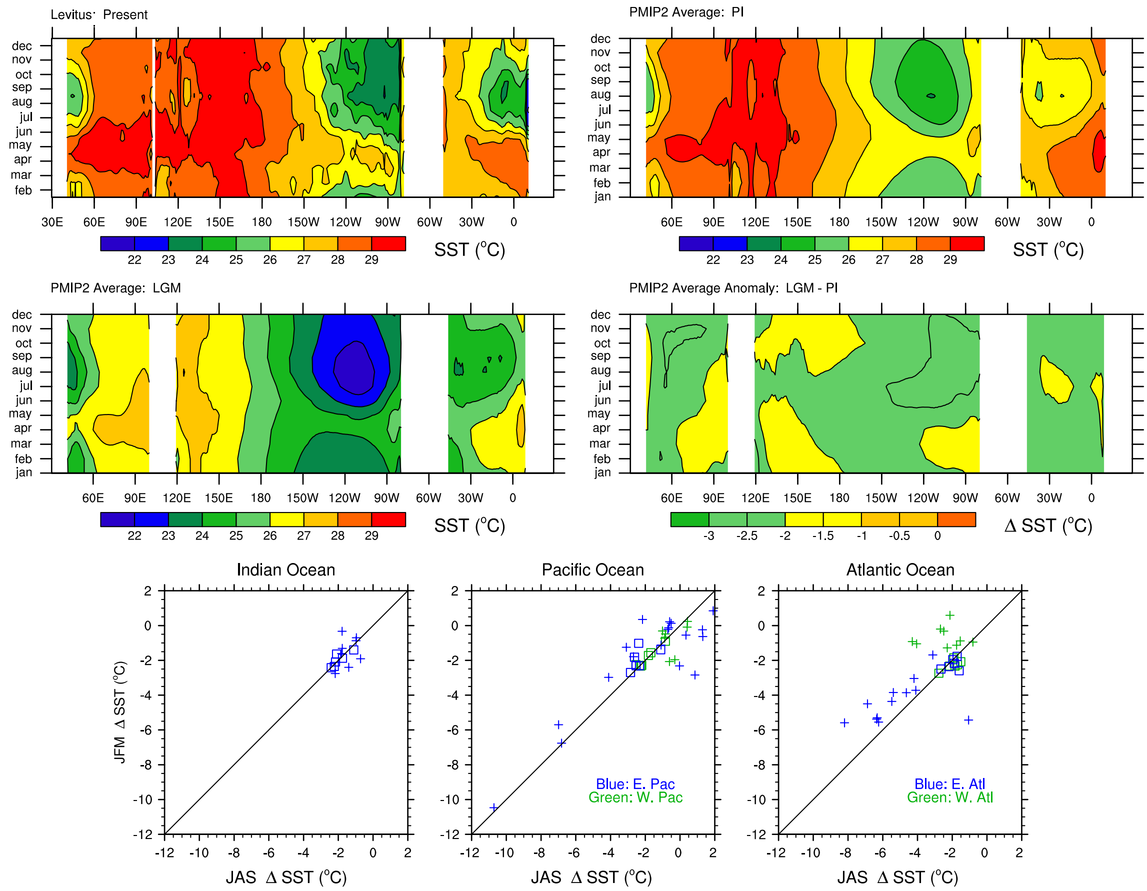

Fig. 7 Top four panels show the seasonal cycle equatorial (5°N–5°S) SST (°C) for observed present-day (Levitus et al. 1998), PMIP2 multi-model mean for PI, PMIP2 multi-mean for LGM, and PMIP2 multi-model mean anomaly LGM minus PI. Bottom three panels show the JFM versus JAS SST anomaly, LGM minus PI, in the Indian, Pacific, and Atlantic equatorial oceans, comparing the PMIP2 model simulations (*square boxes*) to proxy estimates based on foraminifera transfer functions (*plus*), (MARGO Project Members 2009). Subregions are defined as W. Pac (150°E–150°W), E. Pac. (150°W–70°W), W. Atl. (70°W–25°W), and E. Atl. (25°W–30°E)

associated with poorly simulated air-sea interaction feedbacks related to the summer monsoon. The flatter equatorial Atlantic thermocline is associated with weaker surface winds than observed. Large and Danabasoglu (2006) suggest that the eastern Pacific bias is related to both an underestimation of stratocumulus cloud cover in these nearshore regions and upwelling favorable surface wind stresses that are too weak.

One interpretation for the pronounced LGM cooling in the eastern tropical Atlantic found in the proxy records is that not only was the intensity of the upwelling stronger at LGM but also the temperature of the upwelled water much colder (Niebler et al. 2003). As shown, the ocean temperature biases suggest large deficiencies in the simulated eastern boundary currents and upwelling in this region (Fig. 6). It is difficult to achieve the correct dynamical response to LGM forcing given that the correct dynamical response is not achieved for present-day forcing. The multi-model mean equatorial ocean temperatures have cooling in excess of 2°C at LGM below the thermocline in the eastern basins, which suggests a large scale response at LGM of much colder mid latitude water penetrating to the equator, but the colder water is not being upwelled to the surface.

4.5 Sensitivity of tropical ocean cooling to season

Part of the model-proxy data disagreement at LGM may also be related to interpretation of the proxy data as representing an annual mean. The Levitus data for present shows large seasonal cycles of tropical SSTs in the eastern Pacific and Atlantic Oceans (Fig. 7). In the tropical eastern Pacific, the PMIP2 PI multi-model mean has coolest SSTs in July–October and warmest SSTs in April–May, in agreement with the observed seasonal cycle. The simulated seasonal minimum of SST, though, is found too far west, at about 110°W in the PMIP2 multi-model mean, while the Levitus data locates this seasonal minimum close to the coast of South America. The WPWP, which shows little seasonal variation, and the Indian Ocean seasonal cycle of

Table 4 Climate sensitivity terms as estimated from PMIP2 LGM simulations and doubled CO_2 simulations

	ΔTS (°C) LGM − PI Global	Q (W/m^2) Ice sheet + sea level LGM	Q (W/m^2) Total LGM	1/α (°C per W/m^2) LGM	ΔTS (°C) 2 × CO_2 Global LGM estimate	ΔTS (°C) 2 × CO_2 Global Slab ocean	ΔTS (°C) 2 × CO_2 Global Transient 1%
ECBilt-CLIO	−3.1	−1.8	−4.5	0.69	2.6	–	1.7
CCSM	−4.5	−2.7	−5.4	0.83	3.1	2.5	1.5
FGOALS	−5.1	−3.5	−6.2	0.82	3.0	–	1.2
HadCM	−5.1	−4.0	−6.7	0.76	2.8	3.3	2.0
IPSL	−3.3	−1.5	−4.2	0.78	2.9	4.4	2.1
MIROC	−3.7	−2.3	−5.0	0.74	2.7	4.0	2.1

The LGM radiative forcing (Q) associated with changed atmospheric concentrations in the greenhouse gases, as prescribed by the PMIP2 protocol, is −2.8 W m^{-2} and associated with changed orbital configuration is +0.1 W m^{-2}. See text for more detail

SSTs are well-simulated in the PMIP2 multi-model mean. The poor simulation of the tropical Atlantic thermocline structure (Fig. 6) results in a similarly poor simulation of the seasonal cycle of SSTs in this basin.

These seasonal cycle features remain in the PMIP2 LGM simulations with relatively little seasonal change in the magnitude of cooling. The largest seasonal cycle of LGM SSTs occurs in the eastern Pacific, the region of the largest seasonal cycle also at PI in the models (Fig. 7). Coldest SSTs occur in the eastern tropical Pacific with LGM SST less than 21°C in July–August. Minimum SSTs in the western tropical Indian Ocean also occur in northern late summer-early fall. The western and central Pacific show little seasonal cycle of SSTs at LGM, similar also to what is observed at modern. The Atlantic basin at LGM shows the largest seasonal cycle of SST in the western portion similar to PI.

The simulated magnitudes of northern winter (JFM) and northern summer (JAS) cooling are similar, as indicated by the individual model estimates all falling on the one-to-one line (Fig. 7 bottom). This agrees well with the MARGO SST cooling estimates from assemblages of planktonic forаmininfera for the Indian and Pacific Oceans, which also scatter about the one-to-one line suggesting little summer versus winter differences in SST cooling in these ocean basins. The data, though, indicates a tendency for greater cooling in northern summer than northern winter (all locations above the one-to-one line) in the tropical Atlantic which none of the PMIP2 LGM simulations capture.

5 Tropical ocean cooling as a measure of climate sensitivity

Global coupled climate models run for future scenarios of increasing atmospheric CO_2 give a range of response of the global average surface temperature. The IPCC AR4 assessment gives the global mean surface temperature change for a doubling of atmospheric CO_2, broadly termed the equilibrium climate sensitivity, as likely in the range of 2–4.5°C (Meehl et al. 2007).

It has been debated whether the global climate sensitivity is equivalent for cold and warm climates (Manabe et al. 1991; Hansen et al. 1997). A global climate sensitivity for cold glacial conditions can be estimated from the difference between PMIP2 simulations of LGM and PI, assuming both to be steady states, from $Q = \alpha\Delta T$, where Q is the radiative forcing, ΔT the global average surface air temperature change, and $1/\alpha$ the climate sensitivity parameter, related to equilibrium climate sensitivity according to $\Delta T_{2x}=Q_{2x}/\alpha$. Both Q and ΔT for LGM are subject to uncertainty, but the advantage is that their changes for the LGM are large.

The total LGM radiative forcing Q is estimated to be from −4.2 to −6.7 W m^{-2}, primarily associated with the large changes in the greenhouse gases and ice sheets included in the PMIP2 simulations (Table 4). The greenhouse gas contribution to the LGM radiative forcing of −2.8 ± 0.5 W m^{-2} is calculated using the IPCC 2001 equations (Ramaswamy et al. 2001; Otto-Bliesner et al. 2006a; Jansen et al. 2007) including uncertainties in these calculations, and uncertainty estimates for the measurements of the greenhouse gas in the ice cores. The majority of this forcing results from the LGM forcing of −2.2 W m^{-2} associated with reduced atmospheric CO_2.

The ice sheet (and increased land with associated sea level lowering) contributions to the radiative forcing vary considerably among the models, ranging from −1.5 to −4.0 W m^{-2} (Crucifix 2006; Crucifix pers. comm.). Taylor et al. (2007) attribute model differences in LGM ice sheet forcing to primarily model differences in the surface albedo formulations and cloud masking effects. The radiative forcing contribution by solar insolation change is small, +0.1 W m^{-2}.

The PMIP2 models give a range of ΔT for LGM of 3.1–5.1°C (Table 4). The PMIP2 LGM simulations thus give estimates for $1/\alpha$ of 0.69–0.83°C per W m^{-2} and a climate sensitivity for doubling of atmospheric CO_2 of 2.6–3.1°C. This range is similar but narrower than the range of equilibrium climate sensitivity estimated for a doubling of CO_2 of 2.5–4.4°C, obtained by the same models when estimated using slab ocean models (Table 4). Three models suggest greater sensitivity and one model less sensitivity to radiative forcings in their LGM simulations as compared to their doubled CO_2 simulations.

This estimate of climate sensitivity is based entirely on PMIP2 climate model results. There is no estimate from proxy data of global mean temperature change at LGM. It has been suggested that cooling in the tropics at LGM estimated from proxy data might be used to constrain climate sensitivity to atmospheric CO_2 concentrations (Lea 2004). In addition, it has been proposed that a comparison of proxy records to climate model simulations may be able to rule out those models that do not fit the proxy range for LGM and thus give too high or too low warming for future scenarios. This method has been shown to be useful for a single model where an ensemble of perturbed-parameter simulations with varying sensitivities to doubled CO_2 can be constrained using parallel perturbed-parameter simulations for the LGM in conjunction with proxy estimates for the LGM (Annan et al. 2005; Schneider von Deimling et al. 2006; Hargreaves et al. 2007).

The question then is whether the same constraints are possible using simulations from many independent climate models. Table 4 gives the warming of global temperature for the PMIP2 models for a doubling of CO_2 in their slab ocean simulations, the standard method for computing climate sensitivity, as well as transient 1% CO_2 increase simulations available for the fully coupled atmosphere-ocean simulations. There is a slight tendency among the PMIP2 models for larger cooling of the tropical SSTs at LGM between 15°S–15°N, for the entire basin and individual ocean basins, in those models that predict greater global warming for a doubling of atmosphere CO_2. In those tropical ocean regions where radiative influences strongly affect sea surface temperatures, e.g. the western Pacific and Indian Oceans, LGM cooling of SSTs shows better agreement with the MARGO foraminifera transfer function estimates in those models that exhibit an equilibrium climate sensitivity for doubled CO_2 of 2.5°C (CCSM) and 3.3°C (HadCM) than those models with greater sensitivities (4°C IPSL and 4.4°C MIROC) (Fig. 5 and Table 4).

6 Discussion and conclusions

The IPCC Third Assessment Report (TAR) included an evaluation of the PMIP atmosphere-only and atmosphere-slab ocean simulations of tropical SST cooling at LGM as compared to proxy indicators. The PMIP simulations using atmosphere-only models and CLIMAP sea surface temperatures (SSTs) gave a tropical ocean cooling (prescribed) of 0.8°C (McAvaney et al. 2001). The inclusion of a thermodynamic slab ocean model increased the range of cooling of the tropical oceans of 0.8–3.4°C.

The PMIP2 models give a range of tropical (15°S–15°N) SST annual-average cooling of 1.0–2.4°C, comparable to the MARGO estimate of annual cooling of 1.7 ± 1°C (MARGO Project Members 2009). The models simulate greater SST cooling in the tropical Atlantic than tropical Pacific, but interbasin and intrabasin variations of cooling are much smaller than those found in the MARGO reconstruction (Rosell-Mele et al. 2004; Barker et al. 2005; Barrows and Juggins 2005; Chen et al. 2005; Kucera et al. 2005b). None of the models reproduce the strong cooling (>6°C) found at some sites. The simulated tropical coolings are relatively insensitive to season, a feature also present in the MARGO reconstruction of LGM SST from assemblages of planktonic foraminifera for the Indian and Pacific Oceans. The data does indicate seasonality in cooling in the equatorial Atlantic, with greater cooling in northern summer than northern winter (Niebler et al. 2003), not captured by the model simulations.

Model deficiencies that produce biases in the simulations of the tropical upwelling and thermocline at PI remain for the LGM and are partly responsible for the more homogeneous spatial and temporal LGM cooling simulated by the models. The PMIP2 models simulate colder ocean temperature changes below the thermocline in these upwelling regions but these colder waters are not upwelled to the surface. Models of resolution used in this study do not adequately resolve coastal upwelling dynamics, particularly in the tropical Atlantic, and this might explain some of the underestimation by the models of pronounced cooling found in records in eastern parts of the tropical basins. Additionally, different proxies could be preferentially recording interannual variation of warm or cold environments (Mix 2006).

A number of mechanisms and feedbacks in the ocean have been proposed for determining the tropical cooling at LGM, and their relative importance vary from model to model. Previous modeling studies produce conflicting conclusions on the role of ocean heat transport with tropical cooling independent of this transport (Webb et al. 1997), resulting from increased transport to the Northern Hemisphere (Ganopolski et al. 1998), and resulting from increased transport to the Southern Hemisphere (Weaver et al. 1998). A detailed comparison of three PMIP2 LGM simulations found that the northward ocean heat transport at low latitudes of the Atlantic increased in all three models, but the reasons for this increase differed (Murakami et al. 2008). In two of the models (CCSM and HadCM), the temperature contrast between the upper and lower limbs of the Atlantic MOC is responsible, while in the other model (MIROC), the velocity changes are important.

Analyses of coupled and slab ocean simulations indicates that ocean dynamics are important for realizing the entire cooling of tropical SSTs. During the first few decades in the spinup of a coupled atmosphere-ocean simulation for LGM, Liu et al. (2002) found that the surface tropical ocean cooled due to the lower glacial CO_2 levels. This initial tropical cooling only accounted for about half of the final cooling, with the rest associated with the upper ocean circulation, particularly the ventilation of the thermocline and intermediate waters from the South Pacific. Similarly, when in CCSM the dynamical ocean model is replaced with a slab ocean model, LGM tropical SST cooling is reduced to −0.9°C, or only about 50% of the cooling indicated in the coupled simulation (Otto-Bliesner et al. 2006a).

Changes in the atmospheric circulation at LGM have also been shown to be important for regional cooling of the tropical oceans. In HadCM3 (Hewitt et al. 2003), cooler LGM SSTs in eastern Pacific were due to stronger easterly component of the trade wind flow and upwelling in this region associated the ridge of high pressure over the Laurentide ice sheet which extends southward over Central America. Seager et al. (2000) found, using a simple box model, that the interaction of increased wind speeds and increased low cloud cover in the tropics could provide an additional 2°C cooling of tropical SSTs. Processes and feedbacks within each of the PMIP2 models vary and thus preclude attributing their differences in the cooling of the tropical oceans at LGM to any one mechanism.

The PMIP2 model results, with the LGM forcings of large continental ice sheets and reduced greenhouse gas concentrations, indicate an equilibrium climate sensitivity of 2.6°–3.1°, which is similar to (though surprisingly narrower than) the range of climate sensitivity estimated for a doubling of CO_2, obtained by the same models when estimated using slab ocean models. Some models suggest greater sensitivity and others less sensitivity to radiative forcings in their LGM simulations as compared to their doubled CO_2 simulations, giving no clear conclusion on whether the climate sensitivity for cold climates is different, or not, from that of warm climates. The agreement of the average tropical SST cooling predicted by the PMIP2 models and estimated from the MARGO data does suggest that the much higher LGM sensitivities found in some pre-PMIP2 coupled simulations should be ruled out.

An underestimation of the tropical ocean cooling at LGM in these simulations might be expected given the omission of forcings associated with changes in dust and other aerosols in the PMIP2 experimental design. Increased atmospheric aerosols (dust primarily) at LGM have been estimated to result in a radiative forcing of at least −1 Wm^{-2} (Claquin et al. 2003), though with large uncertainties due to the difficulty in estimating this term even for present. Schneider von Deimling et al. (2006) used model simulations with CLIMBER-2 to estimate that dust would cool tropical SSTs an additional 0.4°–0.9°C in a model with climate sensitivity of 1.5°–4.5°C. Dust loadings in the tropics are not spatially uniform (Mahowald et al. 2006). Increases in atmospheric dust loading over the equatorial oceans at LGM might be important for explaining some of the regional cooling indicated by the MARGO reconstruction.

Our understanding can be further improved using an integrated approach of proxy data and climate models to reconstruct climate change and sensitivity (Trenberth and Otto-Bliesner 2003; Rosenthal and Broccoli 2004). LGM simulations with AOGCMs are an important test of models when combined with syntheses of data reconstructions for LGM. Data reconstructions need to further explore the depth, seasonal, and possibly interannual variations of the proxies being used to estimate past state of the oceans and land surface and calibration uncertainties associated with each proxy. Those proxy signals which identify robust regional changes as compared to more local changes should be combined with model syntheses to understand changes in phenomena such as El Niño-Southern Oscillation and its remote teleconnections.

Acknowledgments The National Center for Atmospheric Research is sponsored by the National Science Foundation. We thank Mark Stevens for the programming of the figures. We acknowledge the international modeling groups for providing their data for analysis, the Laboratoire des Sciences du Climat et de l'Environnement for collecting and archiving the model data. The PMIP2/MOTIF Data Archve is supported by CEA, CNRS, the EU project MOTIF and the Programme National d'Etude de la Dynamique du Climat. The MARGO working group acknowledges support from IMAGES and the Fundació Abertis, Barcelona, for the final synthesis meeting and the WDC-MARE (PANGAEA) to archive the LGM proxy data set.

References

Annan JD, Hargreaves JC, Ohgaito R, Abe-Ouchi A, Emori S (2005) Efficiently constraining climate sensitivity with paleoclimate simulations. SOLA 1:181–184. doi:10.2151/sola.2005-047

Ballantyne AP, Lavine M, Crowley TJ, Liu J, Baker PB (2005) Meta-analysis of tropical surface temperatures during the last glacial maximum. Geophys Res Lett 32:L05712. doi:05710.01029/02004GL021217

Bard E (2001) Comparison of alkenone estimates with other paleotemperature proxies. Geochem Geophys Geosys 2:1002 2000GC000050

Barker S, Cacho I, Benway H, Tachikawa K (2005) Planktonic foraminiferal Mg/Ca as a proxy for past oceanic temperatures: a methodological overview and data compilation for the last glacial maximum. Quat Sci Rev 24:821–834. doi:10.1016/j.quascirev.2004.07.016

Barrows TT, Juggins S (2005) Sea-surface temperatures around the Australian margin and Indian Ocean during the last glacial maximum. Quat Sci Rev 24:1017–1047. doi:10.1016/j.quascirev.2004.07.020

Bendle J, Rosell-Mele A (2004) Distributions of U_{37}^{K} and $U_{37}^{K'}$ in the surface waters and sediments of the Nordic Seas: implications for paleoceanography. Geochem Geophys Geosys 5:Q11013. doi:11010.11029/12004GC000741

Berger AL (1978) Long-term variations of caloric insolation resulting from the earth's orbital elements. Quat Res 9:139–167. doi:10.1016/0033-5894(78)90064-9

Braconnot P, Otto-Bliesner BL, Harrison SP, Joussaume S, Peterchmitt J-Y, Abe-Ouchi A, Crucifix M, Fichefet T, Hewitt CD, Kageyama M, Kitoh A, Loutre MF, Marti O, Merkel U, Ramstein G, Valdes PJ, Weber SL, Yu Y, Zhao Y (2007) Results of PMIP2 coupled simulations of the mid-holocene and last glacial maximum—part 1: experiments and large-scale features. Clim Past 3:261–277

Chen M-T, Huang C-C, Pflaumann U, Waelbroeck C, Kucera M (2005) Estimating glacial western Pacific sea-surface temperature: methodological overview and data compilation of surface sediment planktic foraminifer faunas. Quat Sci Rev 24:1049–1062. doi:10.1016/j.quascirev.2004.07.013

Claquin T, Roelandt C, Kohfeld KE, Harrison SP, Tegen I, Prentice IC, Balkanski Y, Bergametti G, Hansson M, Mahowald N, Rodhe H, Schulz M (2003) Radiative forcing of climate by ice-age atmospheric dust. Clim Dyn 20:193–202

CLIMAP project members (1981) Seasonal reconstructions of the earth's surface at the last glacial maximum, Geological Society of America Map and Chart Series MC-36

Conte MH, Weber JC, King LL, Wakeham SG (2001) The alkenone temperature signal in western North Atlantic surface waters. Geochim Cosmochim Acta 65:4275–4287

Conte MH, Weber JC, Ralph N (1998) Episodic particle flux in the deep Sargasso Sea: an organic geochemical assessment. Deep Sea Res Part I 45:1819–1841

Crucifix M (2006) Does the last glacial maximum constrain climate sensitivity? Geophys Res Lett 33:L18701. doi:18710.11029/12006GL027137

Dallenbach A, Blunier T, Flückiger J, Stauffer B, Chappellaz J, Raynaud D (2000) Changes in the atmospheric CH_4 gradient between Greenland and Antarctica during the last glacial and the transition to the holocene. Geophys Res Lett 27:1005–1008

Deser C, Capotondi A, Saravanan R, Phillips A (2006) Tropical Pacific and Atlantic climate variability in CCSM3. J Clim 19:2451–2481

Developers K-1 (2004) K-1 coupled model (MIROC) description. In: Hasumi H, Emori S (eds) K-1 Tech. Report No. 1, Center for Climate System Research, University of Tokyo

Farrera I, Harrison SP, Prentice IC, Ramstein G, Guiot J, Bartlein PJ et al (1999) Tropical climates at the last glacial maximum: a new synthesis of terrestrial palaeoclimate data. I. Vegetation, lake-levels and geochemistry. Clim Dyn 15:823–856

Fleming K et al (1998) Refining the eustatic sea-level curve since the last glacial maximum using far–and intermediate–field sites. Earth Planet Sci Lett 163:327–342

Flückiger J, Dallenbach A, Blunier T, Stauffer B, Stocker TF, Raynaud D, Barnola J-M (1999) Variations in atmospheric N_2O concentration during abrupt climatic changes. Science 285:227–230

Ganopolski A, Rahmstorf S, Petoukhov V, Claussen M (1998) Simulation of modern and glacial climates with a coupled global model of intermediate complexity. Nature 391:351–356

Gordon C, Cooper C, Senior CA, Banks HT, Gregory JM, Johns TC, Mitchell JFB, Wood RA (2000) The simulation of SST, sea ice extents and ocean heat transports in a version of the Hadley Centre coupled model without flux adjustments. Clim Dyn 16:147–168

Hansen J, Sato M, Ruedy R (1997) Radiative forcing and climate response. J Geophys Res 102:6831–6864

Hargreaves JC, Abe-Ouchi A, Annan JD (2007) Linking glacial and future climates through an ensemble of GCM simulations. Clim Past 3:77–87

Hewitt CD, Broccoli AJ, Mitchell JFB, Stouffer RJ (2001) A coupled model study of the last glacial maximum: was part of the North Atlantic relatively warm? Geophys Res Lett 28:1571–1574

Hewitt CD, Stouffer RJ, Broccoli AJ, Mitchell JFB, Valdes PJ (2003) The effect of ocean dynamics in a coupled GCM simulation of the last glacial maximum. Clim Dyn 20:203–218

Jansen E, Overpeck J, Briffa KR, Duplessy J-C, Joos F, Masson-Delmotte V, Olago D, Otto-Bliesner B, Peltier WR, Rahmstorf S, Ramesh R, Raynaud D, Rind D, Solomina O, Villalba R, Zhang D (2007) Palaeoclimate. In: Solomon S, Qin D, Manning M, Chen Z, Marquis M, Averyt KB, Tignor M, Miller HL (eds) Climate change 2007: the physical science basis. Contribution of working group I to the fourth assessment report of the intergovernmental panel on climate change. Cambridge University Press, Cambridge, pp 433–497

Kim S-J, Flato GM, Boer GJ (2003) A coupled climate model simulation of the last glacial maximum, part 2: approach to equilibrium. Clim Dyn 20:635–661

Kitoh A, Murakami S (2002) Tropical Pacific climate at the mid-Holocene and the last glacial maximum simulated by a coupled ocean-atmosphere general model. Paleoceanography 17. doi:10.1029/2001PA000724

Kucera M, Rosell-Mele A, Schneider RR, Waelbroeck C, Weinelt M (2005a) Multiproxy approach for the reconstruction of the glacial ocean surface (MARGO). Quat Sci Rev 24:813–819

Kucera M, Weinelt M, Kiefer T, Pflaumann U, Hayes A, Weinelt M, Chen M-T, Mix AC, Barrows TT, Cortijo E, Duprat J, Juggins S, Waelbroeck C (2005b) Reconstruction of sea-surface temperatures from assemblages of planktonic foraminifera: multi-technique approach based on geographically constrained calibration data sets and its application to glacial Atlantic and Pacific Oceans. Quat Sci Rev 24:951–998

Large WG, Danabasoglu G (2006) Attribution and impacts of upper ocean biases in CCSM3. J Clim 19:2325–2346

Lea DW (2004) The 100,000 year cycle in tropical SST, greenhouse forcing, and climate sensitivity. J Clim 17:2170–2179

Lee KE, Schneider R (2005) Alkenone production in the upper 200 m of the Pacific Ocean. Deep Sea Res Part I 52:443–456

Levitus S, Boyer TP, Conkwright M, Johnson D, O'Brian T, Antonov JI, Stephens C, Gelfield R (1998) Introduction. World Ocean Database 1998. NOAA Atlas NESDIS, vol I, 18:346

Liu Z, Shin S, Otto-Bliesner BL, Kutzbach JE, Brady EC, Lee DE (2002) Tropical cooling at the last glacial maximum and extratropical ocean ventilation. Geophys Res Lett 29. doi:10.1029/2001GL013938

Mahowald NM, Muhs DR, Levis S, Rasch PJ, Yoshioka M, Zender CS, Liu C (2006) Change in atmospheric mineral aerosols in response to climate: last glacial period, preindustrial, modern, and doubled carbon dioxide climates. J Geophys Res 111:D10202. doi:10210.11029/12005JD006653

Manabe S, Stouffer RJ, Spelman MJ, Bryan K (1991) Transient responses of a coupled ocean-atmosphere model to gradual changes of atmospheric CO_2. Part I: annual mean response. J Clim 4:785–818

MARGO Project Members (2009) Constraints on the magnitude and patterns of ocean cooling at the last glacial maximum. Nat Geosci (in press)

Marti O et al (2005) The new IPSL climate system model: IPSL-CM4. Note du Pole de Modelisation no 26, Institut Pierre Simon

Laplace des Sciences de l'Environnement Global. http://dods.ipsl.jussieu.fr/omamce/IPSLCM4/DocIPSLCM4/FILES/socIPSLCM4.pdf

McAvaney BJ, Covey C, Joussaume S, Kattsov V, Kitoh A, Ogana W, Pitman AJ, Weaver AJ, Wood RA, Zhao Z-C (2001) Model evaluation. In: Houghton JT et al (eds) Climate change 2001: the scientific basis. Contribution of working group I to the third assessment report of the intergovernmental panel on climate change. Cambridge University Press, Cambridge, pp 471–525

Meehl GA, Stocker TF, Collins WD, Friedlingstein P, Gaye AT, Gregory JM, Kitoh A, Knutti R, Murphy JM, Noda A, Raper SCB, Watterson IG, Weaver AJ, Zhao Z-C (2007) Global climate projections. In: Solomon S, Qin D, Manning M, Chen Z, Marquis M, Averyt KB, Tignor M, Miller HL (eds) Climate change 2007: the physical science basis. Contribution of working group I to the fourth assessment report of the intergovernmental panel on climate change. Cambridge University Press, Cambridge, pp 747–845

Mix AC (2006) Running hot and cold in the eastern equatorial Pacific. Quat Sci Rev 25:1147–1149

Mix AC, Bard E, Schneider R (2001) Environmental processes of the ice age: land, oceans, glaciers (EPILOG). Quat Sci Rev 20:627–657

Mix AC, Morey AE, Pisias NG, Hostetler SW (1999) Foraminiferal faunal estimates of paleotemperature: circumventing the no-analog problem yields cool ice age tropics. Paleoceanography 14:350–359

Monnin E, Indermuhle A, Dallenbach A, Flückiger J, Stauffer B, Stocker TF, Raynaud D, Barnola JM (2001) Atmospheric CO_2 concentrations over the last glacial termination. Science 291:112–114

Mueller PJ, Fischer G (2001) A 4 year sediment trap record of alkenones from the filamentous upwelling region off Cape Blanc, NW Africa and a comparison with distributions in underlying sediments. Deep Sea Res Part I 48:1877–1903

Mueller PJ, Kirst G, Ruhland G, von Storch I, Rosell-Mele A (1998) Calibration of the alkenone paleotemperature index $U_{37}^{K'}$ based on core-tops from the Eastern South Atlantic and the global ocean (60N–60S). Geochim Cosmochim Acta 62:1757–1772

Murakami S, Ohgaito R, Abe-Ouchi A, Crucifix M, Otto-Bliesner B (2008) Global scale energy and freshwater balance in glacial climate: a comparison of three PMIP2 LGM simulations. J Clim 21:5008–5033

Niebler H-S, Arz HW, Donner B, Mulitza S, Patzold J, Wefer G (2003) Sea surface temperatures in the equatorial and South Atlantic Ocean during the last glacial maximum (23–19 ka). Paleoceanography 18:1069. doi:1010.1029/2003PA000902

Otto-Bliesner BL, Brady EC, Clauzet G, Tomas R, Levis S, Kothavala Z (2006a) Last glacial maximum and Holocene climate in CCSM3. J Clim 19:2526–2544

Otto-Bliesner BL, Tomas R, Brady EC, Kothavala Z, Clauzet G, Ammann C (2006b) Climate sensitivity of moderate and low resolution versions of CCSM3 to preindustrial forcings. J Clim 19:2567–2583

Peltier WR (2004) Global glacial isostasy and the surface of the ice-age Earth: the ICE-5G (VM2) model and GRACE. Annu Rev Earth Planet Sci 32:111–149

Peltier WR, Solheim LP (2004) The climate of the Earth at last glacial maximum: statistical equilibrium state and a mode of internal variability. Quat Sci Rev 23:335–357

Pflaumann U et al (2003) Glacial North Atlantic: sea-surface conditions reconstructed by GLAMAP 2000. Paleoceanography 18:1065.doi:1010.1029/2002PA000774

Pinot S, Ramstein G, Harrison SP, Prentice IC, Guiot J, Stute M, Joussaume S (1999) Tropical paleoclimates at the last glacial maximum: comparison of paleoclimate modeling intercomparison project (PMIP) simulations and paleodata. Clim Dyn 15:857–874

Prahl FG, Popp BN, Karl DM, Sparrow MA (2005) Ecology and biogeochemistry of alkenone production at station ALOHA. Deep Sea Res Part I 52:699–719

Ramaswamy V, Boucher O, Haigh J, Hauglustaine D, Haywood J, Myhre G, Nakajima T, Shi GY, Solomon S (2001) Radiative forcing of climate change. In: Houghton JT, Ding Y, Griggs DJ, Noguer M, van der Linden PJ, Dai X, Maskell K, Johnson CA (eds) Climate change 2001: the scientific basis. Contribution of working group I to the third assessment report of the intergovernmental panel on climate change. Cambridge University Press, New York, p 881

Rosell-Mele A, Bard E, Emeis K–C, Greiger B, Hewitt CD, Muller PJ, Schneider RR (2004) Sea surface temperature anomalies in the oceans at the LGM estimated from the alkenone-$U_{37}^{K'}$ index: comparison with GCMs. Geophys Res Lett 31. doi:10.1029/2003GL018151

Rosenthal Y, Broccoli AJ (2004) In search of paleo-ENSO. Science 304:219–221

Schneider von Deimling T, Held H, Ganopolski A, Rahmstorf S (2006) Climate sensitivity estimated from ensemble simulations of glacial climate. Clim Dyn 27:149–163

Seager R, Clement AC, Cane MA (2000) Glacial cooling in the tropics: exploring the roles of tropospheric water vapor, surface wind speed, and boundary layer processes. J Atmos Sci 57:2144–2157

Shin SI, Liu Z, Otto-Bliesner BL, Brady EC, Kutzbach JE, Harrison SP (2003) A simulation of the last glacial maximum climate using the NCAR CSM. Clim Dyn 20:127–151

Taylor KE, Crucifix M, Braconnot P, Hewitt CD, Doutriaux C, Webb MJ, Broccoli AJ, Mitchell JFB (2007) Estimating shortwave radiative forcing and response in climate models. J Clim 20:2530–2543

Trenberth KE, Otto-Bliesner BL (2003) Toward integrated reconstruction of past climates. Science 300:589–591

Weaver AJ, Eby M, Fanning AF, Wiebe EC (1998) Simulated influence of carbon dioxide, orbital forcing and ice sheets on the climate of the last glacial maximum. Nature 394:847–853

Webb RS, Lehman SJ, Rind D, Healy R, Sigman D (1997) Influence of ocean heat transport on the climate of the last glacial maximum. Nature 385:695–699

Weber SL, Drijhout SS (2007) Stability of the Atlantic meridional overturning circulation in the last glacial maximum climate. Geophys Res Lett 34:L22706. doi:22710.21029/22007GL031437

Weber SL, Drijhout SS, Abe-Ouchi A, Crucifix M, Eby M, Ganopolski A, Murakami S, Otto-Bliesner BL, Peltier WR (2007) The modern and glacial overturning circulation in the Atlantic Ocean in PMIP coupled model simulations. Clim Past 3:51–64

Yokoyama Y, Lambeck K, De Deckker P, Johnston P, Fifield LK (2000) Timing of the last glacial maximum from observed sea-level minima. Nature 406:713–716

Yu Y, Zhang Z, Guo Y (2004) Global coupled ocean-atmosphere general circulation models in LASG/IAp. Adv Atmos Sci 21:444–455